Phase-Separation Mechanism and Corresponding Final Morphologies of Thermoset Blends Based on Unsaturated Polyester and Low-Molar-Weight Saturated Polyester

N. Boyard, M. Vayer, Ch. Sinturel, R. Erre

Centre de Recherche sur la Matière Divisée, 1 B Rue de la Férollerie, 45071 Orleans Cedex 02, France

Received 6 February 2004; accepted 11 September 2004
DOI 10.1002/app.21392
Published online in Wiley InterScience (www.interscience.wiley.com).

ABSTRACT: The final morphology of cured blends based on unsaturated polyester, styrene, and low-molar-weight saturated polyester as a low profile additive (LPA) was investigated with atomic force microscopy and scanning electron microscopy. The observed structure was compared to those obtained with widely used poly(vinyl acetate) (PVAc). On the surface and in the bulk, a network of particles, ranging in size from 50 to 60 nm, was observed with saturated polyester as an LPA. The influence of the molar weight and LPA content was investigated. To determine the mechanism of formation of such a morphology, *in situ* experiments were carried out to elucidate the phase-separation mechanism. Small-angle laser light scattering and small-angle neutron scattering experiments were performed on ternary blends containing PVAc and saturated polyester, respectively. The first stage of spinodal decomposition was observed in both cases. Within our experimental conditions, gelation froze further evolution and led to a two-phase cocontinuous structure that imposed the final morphology characteristics. In particular, the period and amplitude of the concentration fluctuations generated during the phase separation played essential roles. © 2005 Wiley Periodicals, Inc. J Appl Polym Sci 95: 1459–1472, 2005

Key words: phase separation; polyesters; microstructure; thermosets

INTRODUCTION

Unsaturated polyester (UP) resins are used in a large number of industrial applications of composite manufacturing processes, such as the compression molding of sheet molding compounds, the injection molding of bulk molding compounds, resin transfer molding, and vacuum-infusion liquid composite molding (Seeman Composite Resin Infusion Molding Process). These resins consist of a prepolymer in solution in a coreactant acting as a diluent and a crosslinking agent, generally styrene (St). For industrial applications, a thermoplastic polymer is added to reduce macroscopic shrinkage (via pore formation) induced by UP/St copolymerization. A low profile additive (LPA) is a type of thermoplastic additive leading to macroscopic shrinkage lower than 0.1% [poly(vinyl acetate) (PVAc) and saturated polyester]. The initial blend is thus a ternary blend of UP, St and LPA, which is initially miscible within the range of compositions used for industrial applications. The thermoplastic additive does not participate in the copolymerization but induces phase separation (the formation of an LPA-rich phase and a UP-rich phase) until gelation or vitrification of the system.[1–6] Two key factors, the LPA-rich phase volume fraction and phase-separation duration (i.e., the time between the onset of phase separation and the gelation), determine the final structure of the cured blend.[2] These morphologies have been extensively studied for UP resins blended with various LPAs.[2,7–13] The connectivity and particle size are influenced by the chemical nature, the molar weight, and the weight percentage of the thermoplastic additive. The morphology is generally described as a particle network resulting either from microgel formation[11,13] aggregated in nodules[13] or from a phase-separation mechanism.[2,9] However, few articles have reported phase-separation dynamics with respect to morphology formation.[2,3]

For multicomponent polymer mixtures, phase separation is due to incompatibility between the polymeric materials and can be induced by the temperature or a chemical reaction. In general, two types of phase-separation dynamics are expected: spinodal decomposition (SD) and nucleation and growth (NG). The mechanism depends on the thermodynamic balance between the two components and especially the quench depth and composition. The NG mechanism refers to metastability (the system is quenched into the metastable region of the phase diagram[1,4]): it results in spherical, dispersed domains, which increase in size

Correspondence to: M. Vayer (marylene.vayer@univ-orleans.fr).
Contract grant sponsor: La Région Centre.
Contract grant sponsor: Menzolit Co.

© 2005 Wiley Periodicals, Inc.

with time. For a phase-separation mechanism driven by SD, a three-dimensional cocontinuous morphology (a branch structure characterized by a high degree of connectivity for both phases) is formed during the early stage of phase separation; this first step is described by the linearized Cahn–Hilliard–Cook theory.[14–17] SD takes place if the mixture is quenched into an unstable zone of the phase diagram. The growth of this cocontinuous morphology originates from a small and periodic fluctuation of composition. The structure tends to increase in size (step 2), and after this self-similar growth, cocontinuity is lost to yield fragmented particles (step 3) and then spherical particles (coarsening process, step 4). The SD mechanism is well documented in the literature.[1,4]

For reactive systems, a reaction implies some changes in the reactant composition and the boundary between the one-phase and two-phase regions in phase diagrams. These changes induce phase separation. Bucknall et al.[18] developed a conceptual model of a dynamic phase diagram to explain the alteration of the phase diagram for a UP/St/PVAc polymerization reaction at a high temperature. For a thermoset system, the phase separation can be furthermore prematurely stopped by gelation and vitrification. Phase separation induced by a UP/St crosslinking reaction observed with LPA is rarely documented[2] because of experimental difficulties related to compositional changes, to phase diagram alteration during crosslinking, and to a high rate of reaction (contrary to epoxy resins[1,19,20]).

Experimental methods that are frequently used to study phase separation in polymer mixtures include optical microscopy[2,3] and time-resolved scattering.[3,20] For example, phase separation during the crosslinking of a UP/St/PVAc ternary blend at 100°C was studied by small-angle laser light scattering (SALLS) and scanning electron microscopy (SEM).[3] It proceeds by a separation of two cocontinuous phases and the formation of a fragmented structure. The case of saturated polyesters as thermoplastic additives has been rarely explored,[2,21,22] although it has been demonstrated that these additives have great potential for industrial applications for which high surface quality is required.[7] To our knowledge, only Li and Lee[2] studied the phase separation of UP/St blended at low temperatures (between 35 and 55°C) with a saturated polyester [weight-average molecular weight (M_w) = 30,000 g mol^{-1}]. They showed by optical microscopy that SD takes place with the formation of an interconnected structure in the first stage. Coarsening and coalescence can be observed in the late stage as a function of the LPA weight percentage. They also demonstrated that phase separation is frozen by the gelation of the thermoset blend.

Within the frame of this work, our aim was to investigate the phase separation and final morphology of a ternary blend based on UP, St, and a low-molar-weight thermoplastic additive. The question of the relationship between the phase-separation mechanism and final morphology was addressed. The effects of different thermoplastic additives (molar weight and concentration) were studied, especially PVAc and low-molar-weight saturated polyester. The final morphology and phase separation were investigated under experimental conditions as close as possible to industrial conditions. The phase separation was studied with SALLS and small-angle neutron scattering [SANS; performed at Laboratoire Leon Brillouin (Laboratoire Commun Commisariat à l'Energie Atomique–Centre National de la Recherche Scientifique)], and the final morphology was analyzed with SEM and atomic force microscopy (AFM).

TABLE I
Characteristics of the Polymers

Symbol	Chemical composition	M_n (g/mol)	M_w (g/mol)
UP	UP	2,700	12,800
LPA1	Saturated polyester	1,140	2,020
LPA2		2,690	6,420
PVAc	PVAc	100,000	—

M_n = number-average molecular weight.

EXPERIMENTAL

Materials

The thermoset blends were composed of (1) a UP prepolymer, (2) a curing agent (St), (3) an LPA, and (4) a polymerization initiator (tertiobutyl perhexanoate ethyl-2). The UP prepolymer was Palapreg P18-03 from DSM Composite Resins (The Netherlands), made from maleic anhydride, propylene glycol, and neopentyl glycol. Resin P18-03 contained 67.5 wt % UP and 32.5 wt % St. The C═C molar ratio (St/UP prepolymer) in the prepared formulations was adjusted to a value of 2.0 by the addition of St. Noncommercial saturated polyesters (denoted LPA1 and LPA2), made and provided by Cray Valley (France), were employed as thermoplastic additives. They were based on adipic acid, propylene glycol, and ethylene glycol. For comparison, PVAc (Neulon 8000) from Dow Chemicals (Switzerland) was used. The molar weights of these polymers, determined by gel permeation chromatography with polystyrene calibration standards, are listed in Table I. All the materials were used as received, without further purification. Tertiobutyl perhexanoate ethyl-2 (1 wt % UP/St) from Peroxide-Chemie GmbH (Germany) was used as a polymerization initiator. The LPA contents were 5, 15, and 25% of the total weight of the ternary blend (UP/St/LPA). The samples are named by the LPA content followed by

the symbol of the LPA. For example, 15% LPA2 corresponds to a sample containing 15 wt % of the LPA2 thermoplastic additive.

To study the final morphologies, cylindrical samples (diameter = 50 mm, thickness = 4 mm) were molded by compression with a Derek press (Germany) in a stainless steel mold. The polished female part was heated at 150°C, and the punching die was heated at 135°C. The pressure applied on the composites was 10 MPa, and the curing time was 100 s.

Instrumentation and procedures

SEM

SEM was carried out on a Hitachi S4200 device combined with an Oxford analyzer controlled by Link Isis software. The electron gun was equipped with a field emission electron source and was operated at 5 keV. The samples were placed in liquid nitrogen for a few minutes to be fractured. SEM was then performed in the secondary electron mode on the carbon-coated fractured samples. Selected samples were etched with methylene chloride for 15–30 min to dissolve the LPA phase on the fractured surfaces for further investigation.

AFM

AFM in the tapping mode was carried out in air with a Nanoscope III from Digital Instruments Corp. The piezo scanner was able to scan with a horizontal range of 150 μm and a vertical range of 7 μm. Microfabricated Si 120-μm-long cantilevers with integrated Si pyramidal tips (10–15 μm high) were used. The resonance frequency was 300–400 kHz. The vertical and lateral resolutions were less than 1.10^{-3} μm.

SANS

SANS experiments were performed at Laboratoire Léon Brillouin on beam line G5-4 with a PAXE spectrometer. We used a wavelength (λ) of 0.7 nm corresponding to an energy of 2 meV and a scattering vector ($\mathbf{q}$) range of 7.0×10^{-3} to 0.1 Å^{-1}. The beam had a diameter of 7 mm. An area detector (64 unit cells × 64 unit cells) positioned at a distance of 5 m allowed the detection of scattered neutrons. Data were summed radially to express the intensity as a function of $\mathbf{q}$, which was defined as $\mathbf{q} = (4\pi/\lambda)\sin\theta$, and were corrected from transmission, sample-holder scattering, and background due to incoherent scattering (electronic noise in the detector was neglected). The scattered intensity [$I(\mathbf{q})$] depended on the fluctuations of the concentrations and the size of the heterogeneous structure:

$$I(\mathbf{q})_1 = (\Delta b)^2 \mathbf{S(q)} \quad (1)$$

where

$$\Delta b = \frac{a_1}{v_2} - \frac{a_2}{v_1}$$

Δb is the contrast length density defined by the difference between the scattering length of phase 1 and the scattering length of phase 2, and $\mathbf{S}(\mathbf{q})$ is the structure factor. v_1 and v_2 represent the partial molar volumes of phases 1 and 2, respectively. a_1 and a_2 represent the length density of phases 1 and 2 respectively.

Small angle laser light scattering (SALLS)

Light scattering experiments were performed on a homemade apparatus (Centre de Mise en Forme des Matèriaux, Ecole des Mines de Paris, Sophia Antipolis, France) with an unpolarized He–Ne laser light (λ = 632.8 nm). The $\mathbf{q}$ range spanned by the instrument was between 1.5×10^5 and 4×10^6 m^{-1}. More details were given by Maugey and Navard.[5] The samples were prepared by the deposition of a droplet of the studied blend on a small glass plate carefully covered by another one to avoid air bubble formation. The samples were placed in a Linkam THM600 (England) sample stage controlled by a Linkam TMS91 temperature controller. The scattering patterns obtained during crosslinking were observed with a white paper sheet as a screen and were recorded with a charged coupled device (CCD) video camera. The scattering patterns were analyzed with image acquisition and analysis software (IPAS-LS) commercialized by LID (Biot, France).

The circular averaging of each radius symmetric scattering pattern was performed to obtain $I(\mathbf{q})$. The intensity at the beginning of the experiment was subtracted from the intensity measured at later times to avoid notably the dark current of a charge-coupling CCD camera. The recording rate was measured to be 16 images/s. The samples were cured at a heating rate of 10°C/min from room temperature to 140°C. This maximal temperature was then kept constant for 5 min.

RESULTS AND DISCUSSION

Study of the phase separation by SALLS

Figure 1 gives two examples of scattering patterns during curing experiments of UP/St blended with 15% PVAc. No light scattering was detected from room temperature to 108°C [Fig. 1(a)], and this indicated that the system was homogeneous at the probed scale. A typical light scattering ring pattern associated with phase separation[3,20] appeared [Fig. 1(b)] at 108°C and became larger and brighter as the temperature increased. Knowing that the ternary blends were miscible at this temperature (noninitiated blends remained homogeneous), we could relate this diffusion

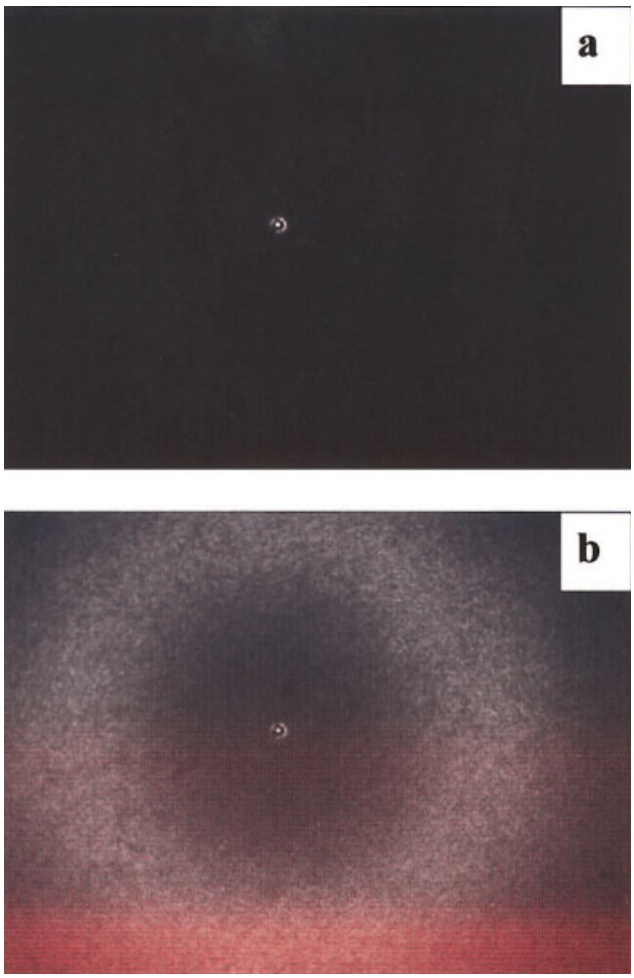

Figure 1 Scattering patterns recorded during the crosslinking of the UP/St/15% PVAc blend: (a) 25 and (b) 108°C.

pattern to a reaction-induced phase separation. The evolution of the $I(\mathbf{q})$ profile is presented in Figure 2 as a function of the $\mathbf{q}$ vector. The profiles were recorded every 6 s. All the scattering profiles were characterized by the existence of a maximum at $\mathbf{q} = \mathbf{q}_{max}$. During the crosslinking, the $\mathbf{q}_{max}$ value remained unchanged. The peak intensity grew quickly to reach a maximum and eventually leveled off. The plot of the logarithm of the maximum intensity (I_{max}) versus the curing time is shown in Figure 3. The logarithm of I_{max} increased linearly as a function of time (during 35 s) and then increased more slowly before reaching a maximal value. Moreover, by plotting the logarithm of the intensity versus the logarithm of $\mathbf{q}$ for high $\mathbf{q}$ values, we show that the slopes of the curves are always -2, as clearly shown in Figure 4. This implies the existence of a diffuse interface.

All these results are evidence of an SD mechanism leading to the development of a structure consisting of two regularly separated cocontinuous phases. Usually, this process has three stages—early, intermediate, and late—which are well depicted in the literature.[1,2,4,5] In the earliest stage, the concentration fluctuations vary slowly with a diffuse interface between the two phases, the scale length is fixed, the peak position remains constant, and its intensity grows exponentially (log I_{max} vs log $\mathbf{q}$ is linear), as predicted by the linear Cahn–Hilliard–Cook theory.[7–10] Then, as concentration fluctuations increase in terms of the period and magnitude, a sharp interface can be observed, $\mathbf{q}_{max}$ shifts to lower values, and I_{max} increases: well-defined domains begin to be formed. At least, because of a too high interfacial energy, the cocontinuous structure is broken (fragmentation), and this stage is dominated by a coarsening process of the domains.

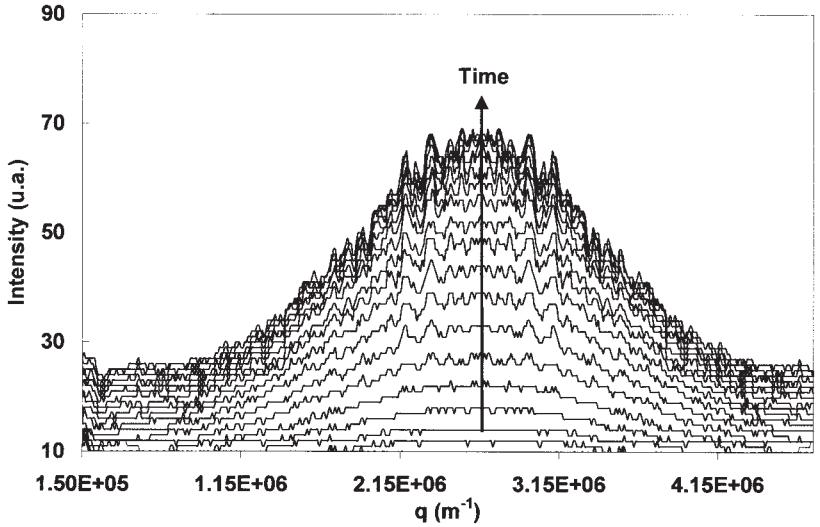

Figure 2 SALLS experiments: evolution of $I = f(\mathbf{q})$ as a function of time during the crosslinking of the UP/St/15% PVAc blend.

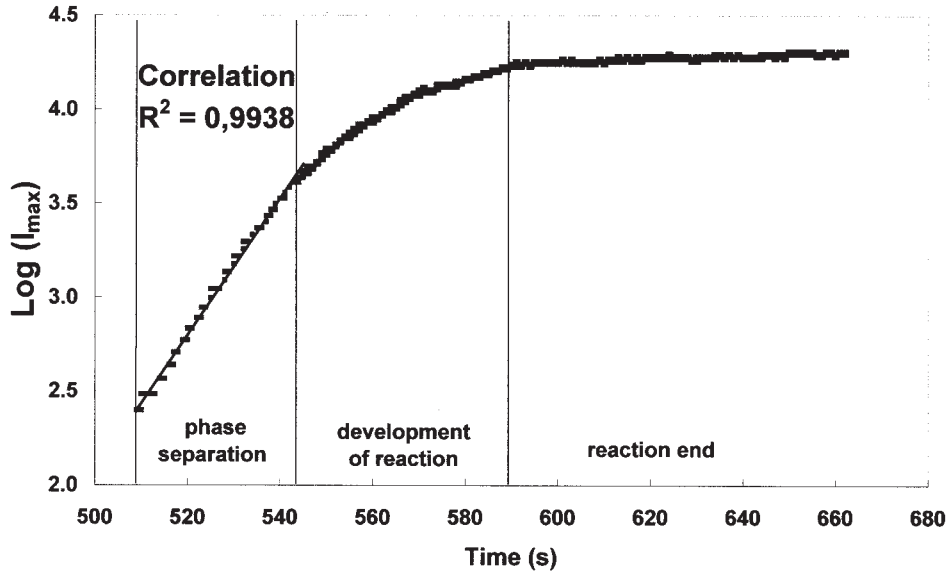

Figure 3 SALLS experiments: evolution of the log I_{max} versus time during the curing of the UP/St/15% PVAc blend.

The experimental results obtained with SALLS led us to conclude that the phase separation observed during the crosslinking of the UP/St/15% PVAc blend followed an SD mechanism frozen by gelation in the earliest stage because of the high reactivity of the UP resin. The gelation for UP/St/thermoplastics occurs at a low conversion degree (between 5 and 10%)[23] and thus interacts with phase separation during the early stage, and this leads to its premature interruption. The characteristic length Λ_{max} can be estimated between 2.3 and 2.4 μm with Bragg's law ($\Lambda_{max} = 2\pi/\mathbf{q}_{max}$). As generally observed for SD,[3] the scattering peak exhibits a broadness, and the Λ_{max} value previously calculated corresponds to a mean value.

SALLS experiments were also carried out for systems containing UP/St blended with 15 or 25% LPA2. A change in the refractive index at 110°C was observed with an optical microscope and indicated the beginning of the reaction, but no scattering patterns were associated with this phenomenon. Phase separation still proceeded but could not be studied within the wave vector range and the wavelength of incident light: the sizes of the domains defined by concentration fluctuations were too small to scatter laser light (λ = 632.8 nm). The SALLS apparatus was not adapted to determine the phase-separation process in this case.

Study of the phase-separation mechanism by SANS

Experiments were performed *in situ* by SANS for different LPA molar weights (LPA1 and LPA2) and con-

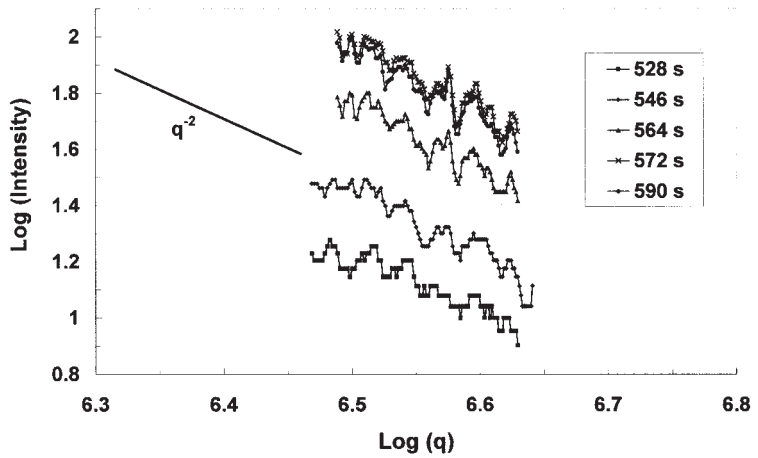

Figure 4 SALLS experiments: evolution of the logarithm of the intensity versus log **q** for high **q** values for different times of curing for the UP/St/15% PVAc blend.

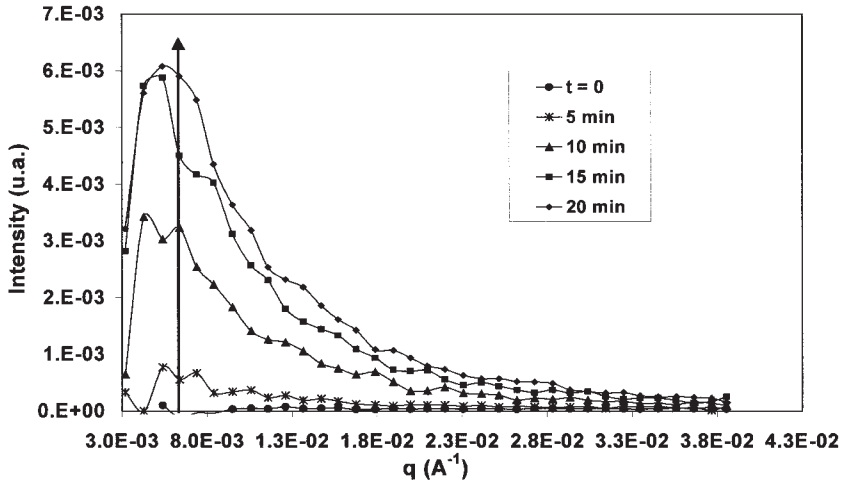

Figure 5 SANS profiles recorded during the beginning of the crosslinking of the UP/St_D/15%LPA1 blend at 70°C. The arrow shows the evolution of the correlation peak.

tents (between 5 and 25 wt %). This technique allowed us to consider smaller sizes of separated domains not possible with SALLS. Deuterated styrene (St_D) was used to obtain a contrast between the polymer phases. The reactions were carried out under conditions such as limited or avoided porosity formation (low curing temperature). The observed scattering was in this case only due to concentration heterogeneities. The absence of pore formation was confirmed by the study of the scattering behavior of the porous material, which exhibited $I(\mathbf{q})$ increased by several orders of magnitude. Furthermore, we restricted this study to the first stage of the reaction, in which no porosity formation could be observed. We indeed demonstrated in a previous work that porosity formation is restricted to the late stage of the reaction.[24] As UP was very reactive under our conditions, a low recording time for the scattering profiles was used. Each scattering pattern was recorded for 5 min during isothermal curing at 70°C. All the samples exhibited the same kind of behavior, with a correlation peak growing at a constant **q** value.

Figure 5 presents the evolution of the scattering profile during the copolymerization of the UP/St_D/15% LPA1 blend. The profiles exhibit a correlation peak for $\mathbf{q} = 5.4 \times 10^{-3}$ Å^{-1}. The associated characteristic length (according to Bragg's law) is $\Lambda_{max} = 117$ nm. During the reaction, the peak grows at a fixed angular position. This behavior is similar to that observed in SALLS during UP/St/PVAc blend crosslinking. After 20 min, the curves superimpose. The slopes of the various curves at high **q** values were also determined. Figure 6 shows that these curves evolve with a $\mathbf{q}^{-2}$ power law for high **q** values, and this means that the interface between separating do-

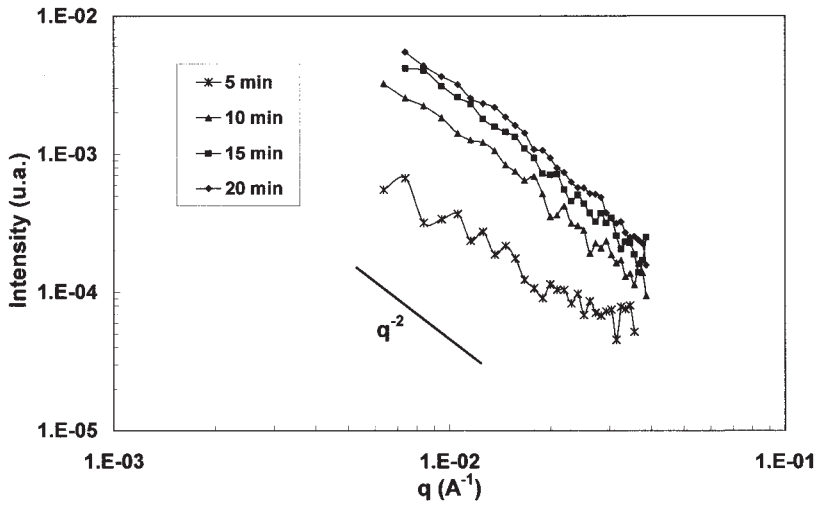

Figure 6 SANS intensity versus **q** (high values) in a logarithmic scale during the curing of the UP/St_D/15%LPA1 ternary blend at 70°C.

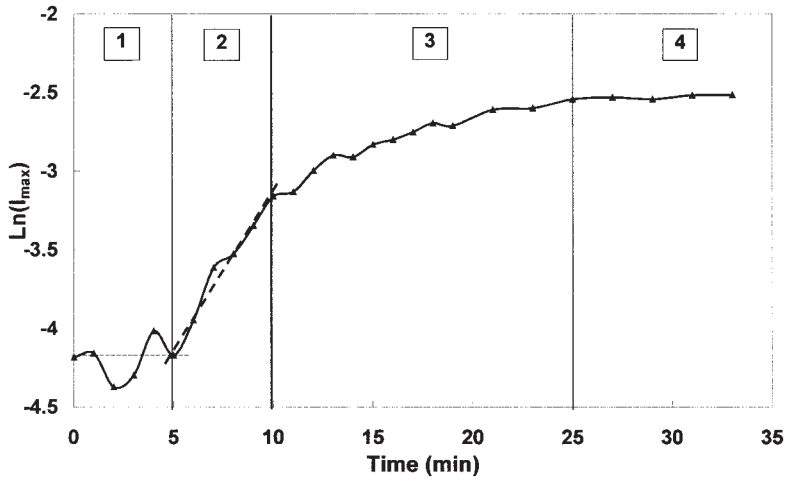

Figure 7 SANS experiments: plot of ln I_{max} as a function of time at $\mathbf{q}_{max}$ values corresponding to the UP/St_D/15%LPA1 blend.

mains was diffuse (low amplitudes of concentration fluctuations). The $\mathbf{q}^{-2}$ behavior observed on all the scattering profiles is proof of SD being frozen in the early stage. The logarithm of the intensity versus time at $\mathbf{q}_{max}$ is shown on Figure 7. Four zones can be distinguished:

1. $I(\mathbf{q})$ is very low, and this indicates that the crosslinking has not begun yet.
2. The curve evolves linearly for 5 min, and this indicates an exponential increase in $I(\mathbf{q})$.
3. The intensity increases more slowly. The phase separation is stopped, and the $I(\mathbf{q})$ evolution is due to the modification of the contrast length occurring in the separated phases (species interdiffusion and further crosslinking).
4. After 25 min, the intensity remains constant, and this indicates that the reaction is ended.

The linear behavior of the logarithm of the intensity at the beginning of the reaction is additional proof of the SD mechanism. The NG process is rejected (this type of phase separation would, moreover, imply an initial slope of the curve for large angles equal to -4).

For the 15% LPA2 blend, the behavior upon curing is rather different. Starting at -2, the slope of the logarithm of the intensity as a function of the logarithm of $\mathbf{q}$ eventually evolves to -4 and suggests that a sharp interface is formed corresponding to high amplitudes of concentration fluctuations (Fig. 8). As no porosity is generated for this conversion degree, this sharp interface has to be related to the interface of LPA-rich and UP-rich phases. The correlation peak has a constant $\mathbf{q}$ position, no coarsening takes place, and a cocontinuous two-phase structure still remains.

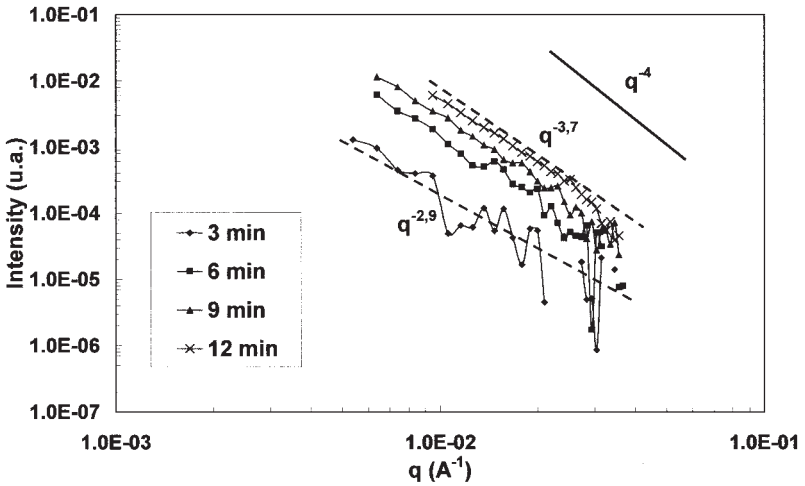

Figure 8 SANS intensity versus $\mathbf{q}$ (high values) in a logarithmic scale during the curing of the UP/St_D/15%LPA2 ternary blend at 70°C.

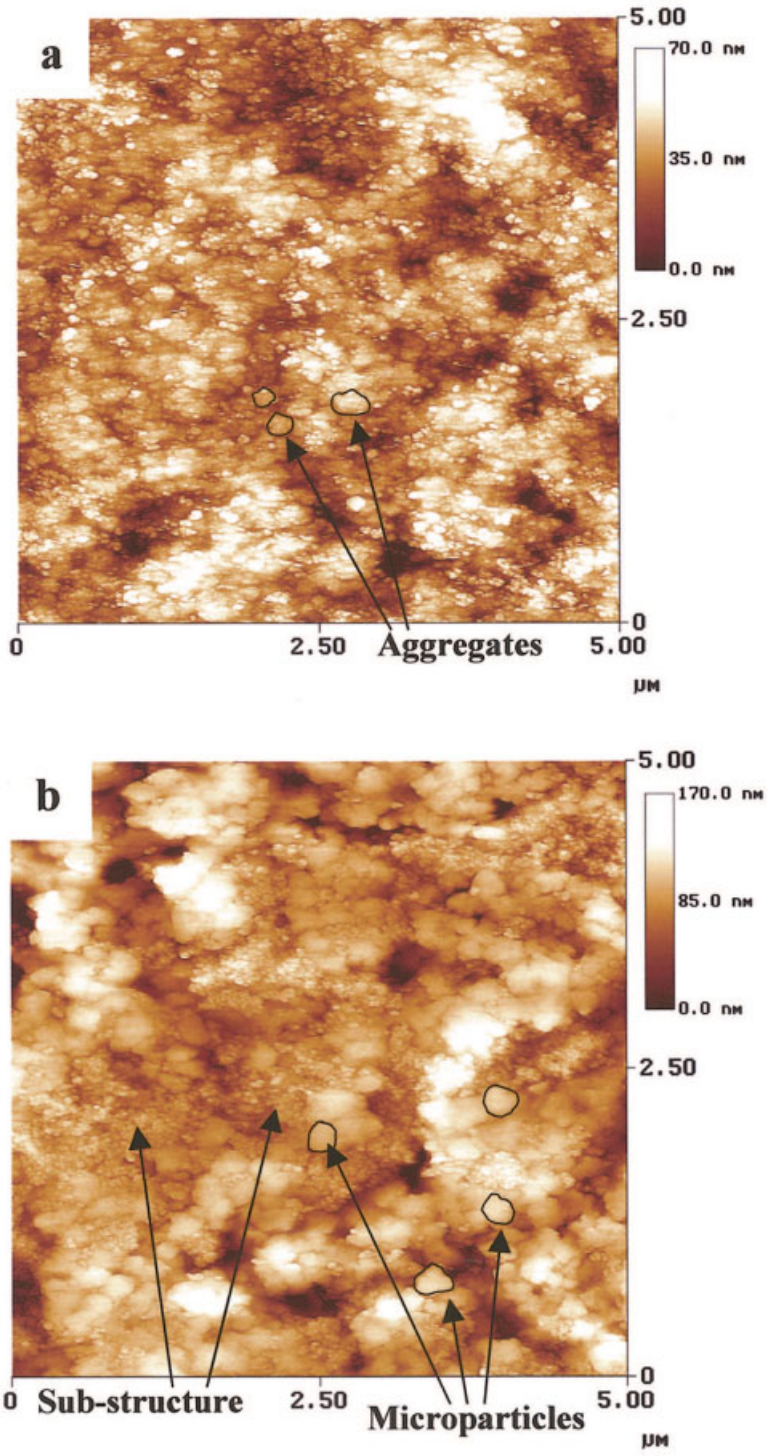

Figure 9 AFM images ($5 \times 5\ \mu m^2$) of (a) 15% LPA2 and (b) PVAc samples.

Final surface and bulk morphologies

Comparison between saturated polyester and PVAc as thermoplastic additive

AFM is a powerful tool for providing pertinent information on the surface topography of cured blends, as displayed in Figure 9(a). The surface of the crosslinked ternary blend was discontinuous, composed of particles named primary particles (also called microgels in the literature) with an average size of 50 nm. These particles collapsed into aggregates (also called nodules) with various sizes (between 200 and 500 nm, depending on the sample). These aggregates were linked together to form a network.

The observation of particles demonstrates that phase separation occurs on the surface during copolymerization (we have verified that no particles exists

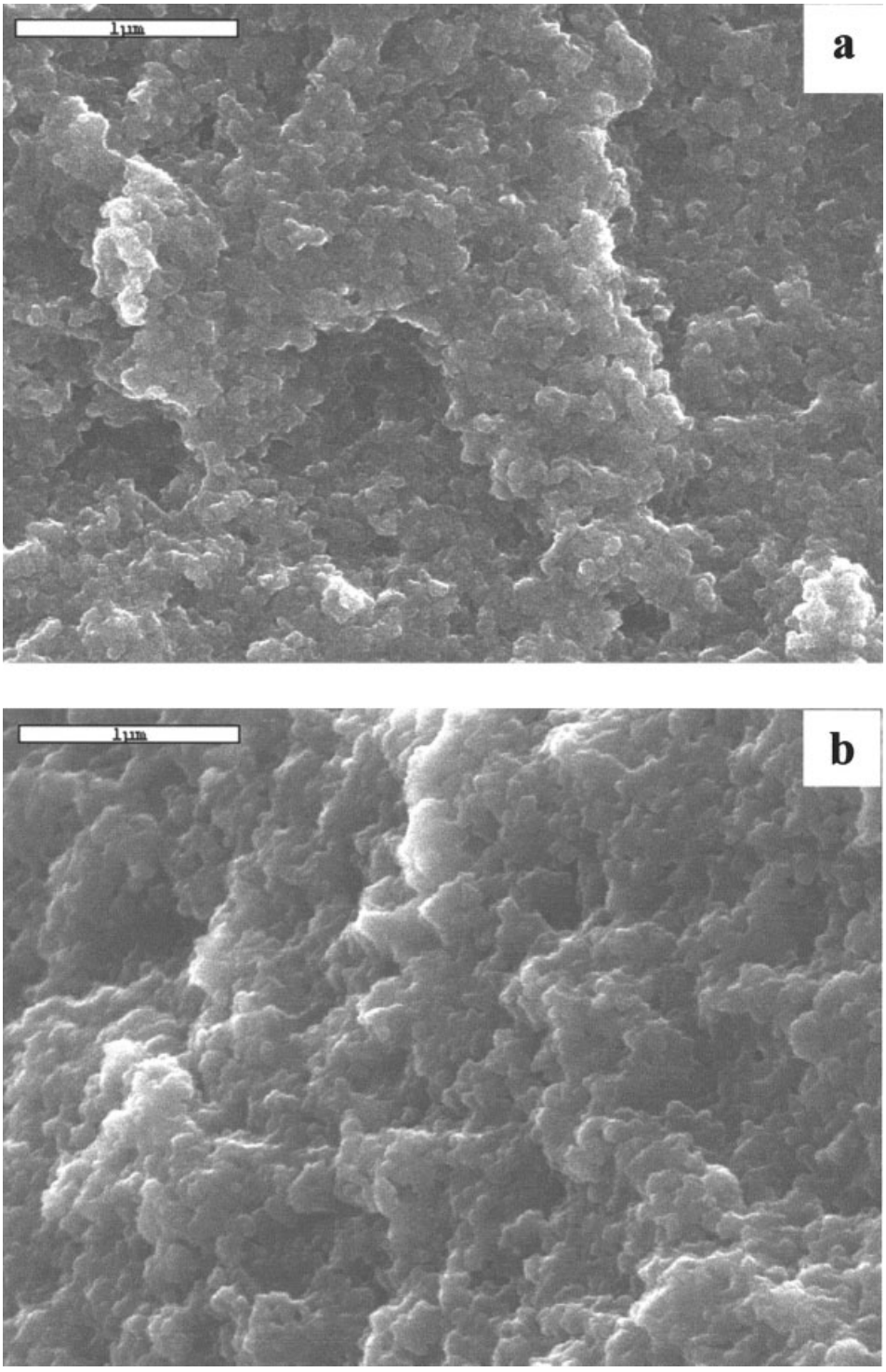

Figure 10 SEM micrographs of a 15% LPA2 sample examined (a) before and (b) after etching with CH_2Cl_2.

on the surface of UP/St-cured samples[19]). The surface morphology observed in this case is radically different from that observed with classical thermoplastics such as PVAc [Fig. 9(b)]. the latter is indeed constituted of microparticles (average size = 500 nm) and a substructure containing primary particles (50–60 nm in size) located around the microparticles. This kind of morphology was already observed by Hsieh and Yu,[3] who suggested that it was the result of two successive phase separations.

The bulk morphology was investigated by SEM on a fractured sample. Figure 10(a) shows the bulk morphology of a 15% LPA2 sample before treatment with CH_2Cl_2. It clearly shows a discontinuous, nodular structure consisting of primary particles with an average size of 80 nm. The particles were linked together in

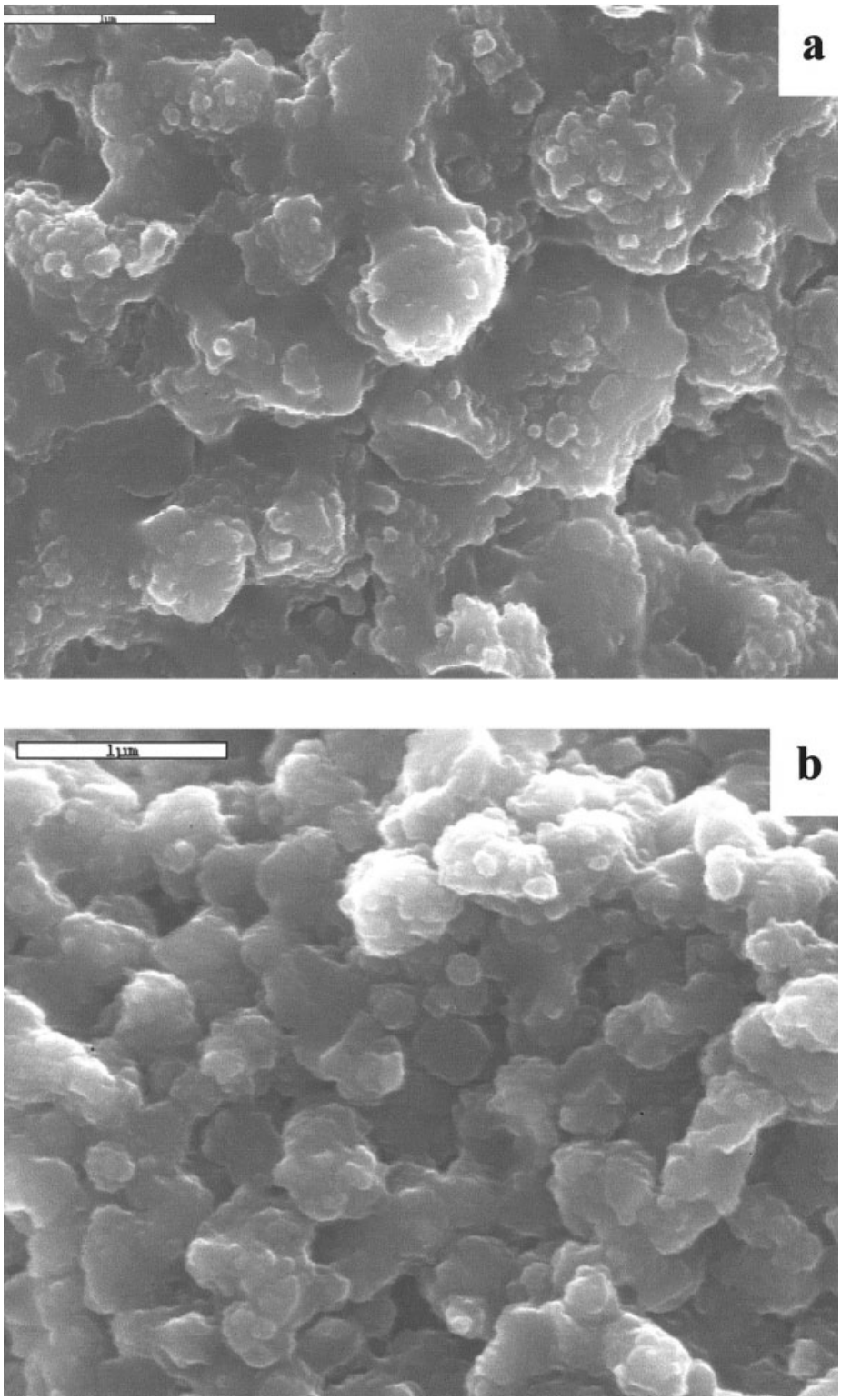

Figure 11 SEM micrographs of a 15% PVAc sample (a) before and (b) after etching with acetone.

aggregates (200 nm) forming a three-dimensional network. The dissolution of LPA with methylene chloride was performed. Figure 10(b) shows the modification of the morphology induced by the treatment with more discernable particles. We conclude that the particles and aggregates consisted of crosslinked UP/St surrounded by an LPA phase. The final morphology can then be described as a cocontinuous, two-phase, nodular structure. The surface and bulk morphologies were similar, and this suggested that these cured mor-

phologies were little affected by the temperature gradient, which might have occurred upon curing within the thickness of the sample.

The bulk morphology was also examined for a 15% PVAc sample [Fig. 11(a)]. Microparticles, with an average size of 550 nm, can be easily observed and correspond to those observed by AFM. Smaller particles (40–70 nm) were located around microparticles. The surface and bulk morphologies appeared to be identical. After the dissolution of PVAc with acetone [Fig. 11(b)], the smaller particles were less numerous, and the network was less compact; this indicated that these particles were principally located in the PVAc-rich phase. These SEM results were re in good agreement with the morphological studies given in the literature.[21,25]

These peculiar structures, observed by AFM and SEM, can be related to the aforementioned characteristics of phase separation. As the UP-rich phase containing the primary particles separates from the phase containing LPA following SD frozen in a bicontinuous structure, LPA finally covers the surface of primary particles. A thermoplastic additive is then considered a segregating agent, which causes much less merging of primary particles and thus retains the identity of the individual primary particles. This interpretation is supported by work reported in the literature.[11,12]

The use of different thermoplastic additives (low-molar-weight saturated polyester or commercial PVAc) induced a strong modification of the final morphology on the surface and in the bulk. This behavior has be related to the difference in the initial miscibility of the blends, which was evaluated with phase diagrams. As shown in Figure 12, phase diagrams obtained for LPA1 and LPA2 exhibit an enlarged miscibility domain in comparison with those for PVAc.[9] We propose that this miscibility difference will lead to different periods of concentration fluctuations for LPA and PVAc during phase separation (Λ_{max} for PVAc = 2.3 μm; Λ_{max} for LPA1 = 117 nm). As phase separation is stopped in the first stage for all blends, it will finally lead to enlarged particles for PVAc. This assumption is consistent with the sizes of the final particles observed by the micrographs of fully cured samples.

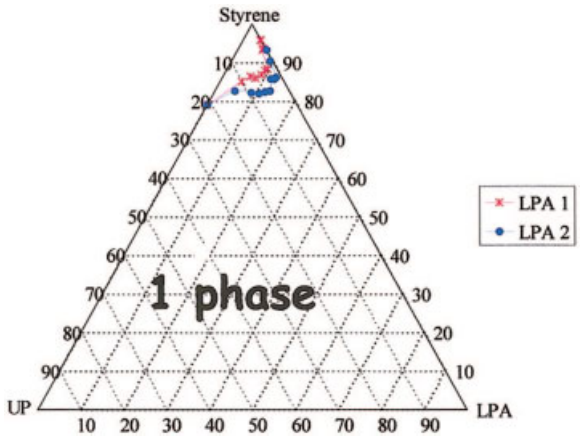

Figure 12 Ternary phase diagram for LPA1 and LPA2 determined at 25°C.

Influence of the molar weight and percentage of saturated polyester on the morphologies

AFM and SEM images are presented in Figures 9(a), 10(a), 13, and 14 for various compositions of LPA1 and LPA2. Table II presents particle sizes and aggregate sizes. The surface and bulk morphologies are sensitive to the LPA content in the ternary blend. The modifications are essentially changes in the compactness and surface homogeneity. With an LPA concentration of 5%, it is difficult to observe particles; the crosslinked network is compact, and the surface is perturbed. With the addition of 15% LPA, the distinction of the primary particles and aggregates is easier, especially with LPA2. The surface aspect is in this case improved because the distribution of the particles is more homogeneous. In the case of 15% LPA1, the changes are not so obvious, and this can be attributed to the lower molar weight of this additive, as will be discussed later. With 25% LPA, the network is less tightly packed, particles are clearly identified, and their sizes increase slightly (Table II). The surface morphology is also more homogeneous. Morphology dependence on the LPA content is related to the segregating effect of LPA described previously. Indeed, a high LPA content favors the individualization of crosslinked UP particles.

The influence of the molar weight of the thermoplastic additive on the morphology can be observed by a comparison of Figures 13 and 14 (AFM and SEM images). For a given amount of LPA, increasing the additive molar weight leads to a more homogeneous nodular structure with highlighted particles. A small increase in the primary particle size can also be noted (Table II). This behavior can be clearly observed for 15 and 25% but is less obvious for 5%. The segregating effect of the LPA is obviously highly dependent on the additive amount. The morphology dependence on the LPA molar weight can be related to the position of the phase separation onset with respect to the gelation, which is known to stop further evolution of phase separation. In our system, gelation occurs for a conversion degree of about 5–10%. Increasing the molar weight of the LPA decreases the miscibility of the LPA and then advances the phase-separation onset (Fig. 12). A longer time of phase separation is then expected and favors the segregating effect of this LPA.

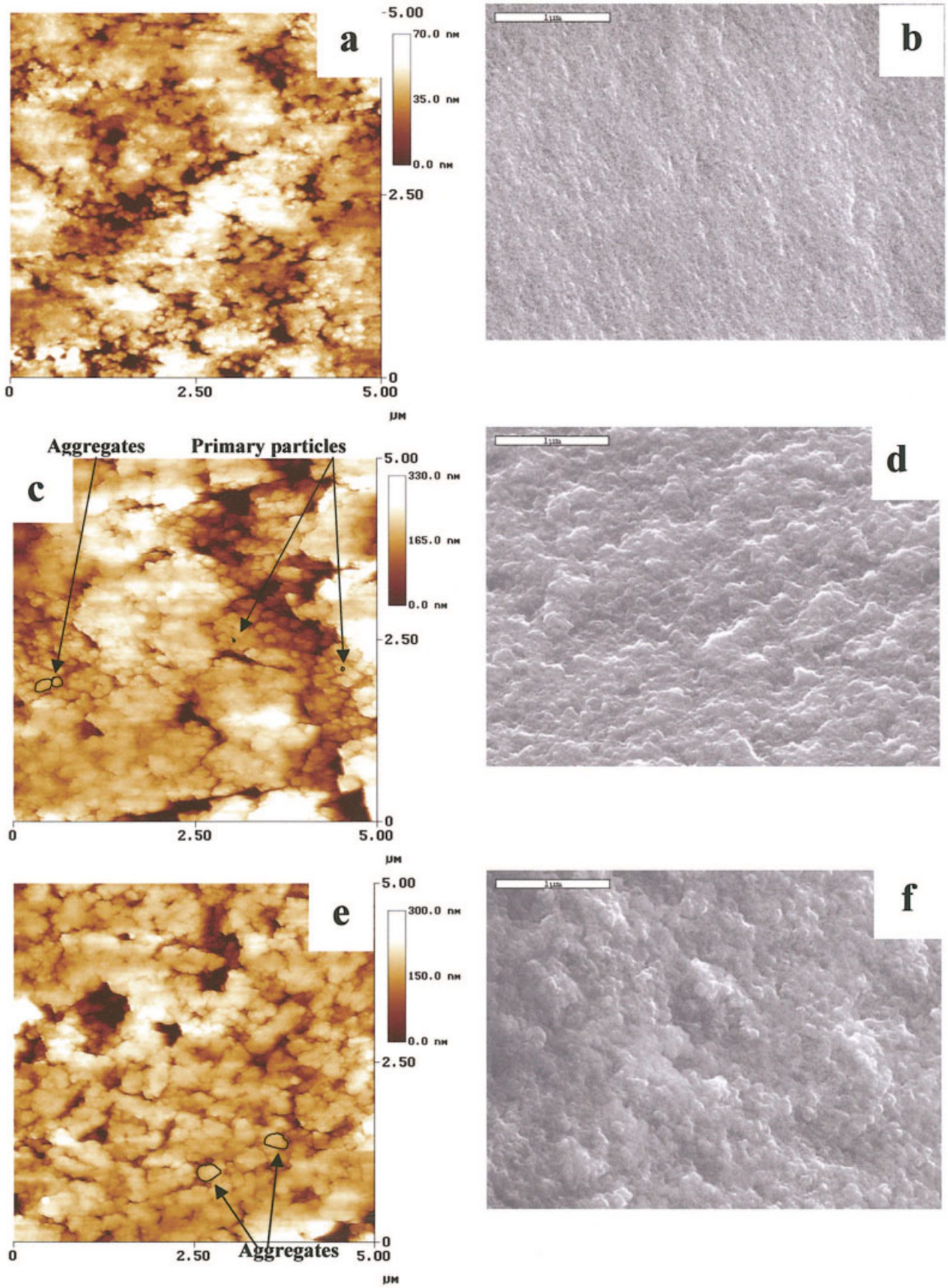

Figure 13 AFM and SEM images of samples containing (a,b) 5, (c,d) 15, and (e,f) 25% LPA1.

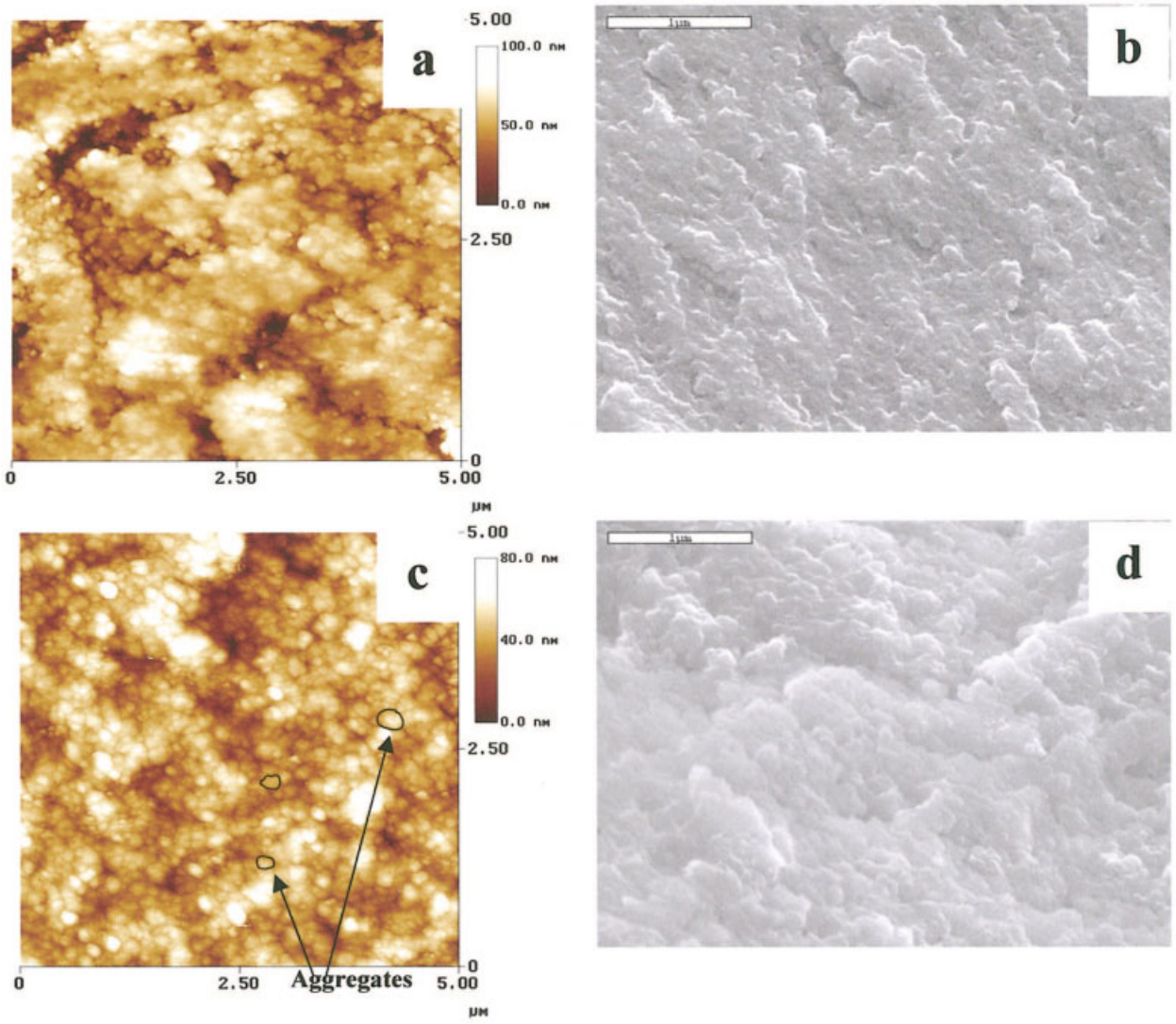

Figure 14 AFM and SEM images of samples containing (a,b) 5 and (c,d) 25% LPA2.

CONCLUSIONS

The final morphology of thermoset polymers based on UP is highly dependent on the characteristics of the thermoplastic additive (chemical composition, molar weight, and amount). In particular, using low-molar-weight saturated polyester leads to a morphology strictly different than that of PVAc. This behavior is related to the phase-separation characteristics. *In situ* experiments (SALLS and SANS) have shown that under our experimental conditions of cure, the phase separation proceeds via SD frozen by gelation in the first stage, and this leads to a cocontinuous biphasic structure. The period and amplitude of the concentration fluctuations are dependent on the characteristics of the thermoplastic additives. These results are correlated to the morphology of the cured systems, for which a two-phase cocontinuous structure has been found with a particle size within the period length of the concentration fluctuations depicted previously.

TABLE II
Sizes of Primary Particles and Aggregates Determined by AFM and SEM

Ternary blend	Primary particles ± 5 (nm)	Aggregates ± 10 (nm)
5% LPA1	40	—
15% LPA1	50–60	150–200
25% LPA1	50–60	200–240
5% LPA2	40–50	—
15% LPA2	40–70	200–250
25% LPA2	60–80	180–230
15% PVAc	50–60	500 (microparticles)

These mean sizes were determined by consideration of 10 5 × 5-μm^2 images and measurement of 15 aggregate and particle sizes for each image.

The authors thank A. Richard for the scanning electron microscopy images, J. Teixeira (Laboratoire Leon Brillouin,

Saclay, France) for the small-angle neutron scattering experiments and much advice, and E. Peuvrel-Disdier (CEMEF, Ecole des Mines de Paris, France) for the small-angle laser light scattering analysis and fruitful discussions.

References

1. Inoue, T. Prog Polym Sci 1995, 20, 119.
2. Li, W.; Lee, L. J. Polymer 2000, 41, 697.
3. Hsieh, Y. N.; Yu, T. L. J Appl Polym Sci 1999, 73, 2413.
4. Bansil, R.; Liao, G. TRIP 1997, 5, 146.
5. Maugey, J.; Navard, P. Polymer 2002, 43, 6829.
6. Schulz, M.; Paul, B. Phys Rev B 1998, 58, 11096.
7. Serre, C.; Vayer, M.; Boyard, N.; Ollive, C.; Erre, R. J Mater Sci 2001, 36, 113.
8. Suspene, L.; Gerard, J.-F.; Pascault, J.-P. Polym Eng Sci 1990, 30, 1585.
9. Suspene, L.; Fourquier, D.; Yang, Y.-S. Polymer 1991, 32, 1593.
10. Vayer, M.; Serré, C.; Boyard, N.; Sinturel, C.; Erre, R. J Mater Sci 2002, 37, 2043.
11. Huang, Y.-J.; Su, C.-C. J Appl Polym Sci 1995, 55, 323.
12. Huang, Y.-J.; Su, C.-C. Polymer 1994, 35, 2397.
13. Yang, Y. S.; Lee, L. J. Polymer 1988, 29, 1793.
14. Cahn, J. W.; Hilliard, J. E. J Chem Phys 1958, 28, 258.
15. Cook, H. E. Acta Metall 1970, 18, 297.
16. Binder, K. J Chem Phys 1983, 79, 6387.
17. Jinnaï, H.; Hasegawa, H.; Hashimoto, T.; Han, C. C. J Chem Phys 1993, 99, 8154.
18. Bucknall, C. B.; Davies, P.; Partridge, I. K. Polymer 1985, 26, 109.
19. Girard-Reydet, E.; Sautereau, H.; Pascault, J.-P.; Keates, P.; Navard, P.; Thollet, G.; Vigier, G. Polymer 1998, 39, 2269.
20. Zheng, Q.; Tan, K.; Peng, M.; Pan, Y. J Appl Polym Sci 2002, 85, 950.
21. Li, W, Lee, L. J. Polymer 2000, 41, 685.
22. Li, W, Lee, L. J. Polymer 2000, 41, 711.
23. Pascault, J. P.; Sautereau, H.; Verdu, J.; Williams, R. J. J. Thermosetting Polymers; Marcel Dekker: New York, 2002.
24. Boyard, N.; Vayer, M.; Sinturel, C.; Erre, R.; Delaunay, D. J Appl Polym Sci 2004, 92, 2976.
25. Huang, Y.-J.; Liang, C.-M. Polymer 1996, 37, 401.